

# Crosslinkable fumed silica-based nanocomposite electrolytes: role of methacrylate monomer in formation of crosslinked silica network

Jeffrey A. Yerian, Saad A. Khan, Peter S. Fedkiw\*

Department of Chemical Engineering, North Carolina State University, Raleigh, NC 27695-7905, USA

Received 19 February 2004; accepted 10 March 2004

## Abstract

The electrochemical and rheological properties of composite polymer electrolytes (CPEs) based on fumed silica with tethered crosslinkable groups are reported. These silica nanoparticles are dispersed in electrolytes consisting of poly(ethylene glycol) dimethyl ether (PEGdm) + lithium bis(trifluoromethanesulfonyl)imide (LiTFSI) to which various methacrylate monomers, such as methyl (MMA), ethyl (EMA), butyl (BMA), *n*-hexyl (HMA), and *n*-dodecyl (DMA) methacrylate, are added. The methacrylate monomer facilitates creation of chemical crosslinks between fumed silica particles and formation of a crosslinked network. In this study, the effects of concentration and alkyl chain length of the monomers on conductivity, dynamic rheology, open-circuit interfacial stability, and cell voltage in lithium–lithium cell cycling are examined. Increasing the length of the monomer alkyl chain enhances both conductivity and elastic modulus of the crosslinked CPE. In contrast, increasing monomer concentration results in higher elastic modulus, but reduced conductivity. Lithium–lithium cell cycling and open-circuit interfacial stability results did not correlate with alkyl chain length. That is, for the lithium–lithium cycling studies, all crosslinked samples exhibit higher half-cycle voltage compared to non-crosslinked samples; however, the open-circuit interfacial stability of CPEs containing BMA and HMA exhibit improved stability compared to the other monomers and the CPE without monomer.

© 2004 Elsevier B.V. All rights reserved.

*Keywords:* Composite polymer electrolyte; Silica nanoparticle; Electrolyte; Rheology

## 1. Introduction

Rechargeable lithium batteries are promising power sources for devices such as electric vehicles, portable electronics, and implantable medical devices, because of their high-energy density and low self-discharge rate. Although significant progress has been made in these batteries, several important factors, especially the low conductivity and chemical stability of the electrolyte, have limited their commercial use. A large portion of electrolyte research focuses on improving the mechanical strength of the electrolyte without sacrificing important electrochemical properties, such as conductivity, lithium transference number, and interfacial stability.

Electrolytes for lithium batteries must have acceptable ionic conductivity ( $>10^{-3} \text{ S cm}^{-1}$  at 25 °C) and should possess a high  $\text{Li}^+$  transference number, i.e., a high ratio

of the charge transported by  $\text{Li}^+$  compared to the total charge transported [1–3]. Electrolytes must be chemically and electrochemically stable, mechanically strong, yet easily processable, safe, and inexpensive [1–6]. Solid polymer electrolytes have been recognized as viable candidates for rechargeable lithium batteries. The use of solid polymer electrolytes would overcome limitations of liquid electrolytes including: lithium dendrite formation, electrolyte leakage, flammable organic solvent, and electrolytic degradation of electrolyte [5,7,8].

Early approaches to solid polymer electrolytes employed high-molecular weight ( $M_n > 10^5$ ) polyethylene oxide (PEO) [9–11]. Linear PEO forms a semi-crystalline electrolyte with reasonable mechanical properties after addition of lithium salts. The crystallites act as crosslinks that make high-molecular PEO dimensionally stable up to the melting point of the salt–polymer complexes ( $\sim 65^\circ\text{C}$ ). However, since conductivity is dominated by the segmental motion of the amorphous polymer, the presence of crystalline phase reduces the room-temperature conductivities to less than  $10^{-5} \text{ S cm}^{-1}$ , which is too low for most practical

\* Corresponding author. Tel.: +1-919-515-3572; fax: +1-919-515-3465.  
E-mail address: [fedkiw@eos.ncsu.edu](mailto:fedkiw@eos.ncsu.edu) (P.S. Fedkiw).

applications [10,11]. Various methods have been devised to inhibit crystallinity and maximize the volume fraction of the amorphous phase in PEO, including: (a) synthesis of PEO-based polymers with modified architectures [1,12–15]; (b) addition of ‘plasticizers’ [10,16–25]; (c) addition of solvents [6,24,26–34]; (d) addition of inorganic fillers such as alumina, silicas, and zeolites [11,14,35–48].

The synthesis of PEO-based polymers with modified architectures has emphasized comb-branched systems, where the “teeth” of the comb are designed to have maximum flexibility and hence high conductivity. However, the mechanical properties of these polymers are poor and require crosslinking to minimize creep. Even for these neat polymer systems, regardless of the polymer structure, the room-temperature conductivity [15] of electrolytes is less than  $5 \times 10^{-5} \text{ S cm}^{-1}$ . The addition of plasticizers to PEO, either as an absorbed liquid or as a plasticizing lithium salt [10,16,23–25], is often used to reduce the glass transition temperature  $T_g$  and increase conductivity to  $5 \times 10^{-4} \text{ S cm}^{-1}$ ; however, such additives often cause a reduction in mechanical properties and a decrease in the interfacial stability with lithium [2,11,49].

Gel electrolytes are two-component systems that are prepared by dispersing liquid solvents (typically, organic carbonates) and/or plasticizers in an electrochemically inert polymer, such as polyacrylonitrile (PAN) and poly(vinylidene fluoride) (PVdF) [12,13,50–53]. Here, the ionic transport is primarily governed by the liquid electrolyte with the polymer providing mechanical support. The ionic conductivity of a gel electrolyte is higher than that of a solid system, but often at the expense mechanical strength. To improve the mechanical properties of the gel, crosslinkable components (e.g., diacrylate compounds) may be added to form networked gel–polymer systems [51,52].

The addition of inorganic fillers to form composite polymer electrolytes (CPEs) decreases the crystallinity in samples prepared from high-molecular weight PEO, thus stabilizing the conductive amorphous phase. Furthermore, the fillers can form self-assembled network structures that provide favorable mechanical properties in low-to-moderate molecular weight electrolyte systems [54–63]. The principal advantage of the self-assembly approach is that it provides significant processing advantages that can lead to reduced-cost electrolytes.

CPEs consisting of low-molecular weight polyethers, lithium salts, and fumed silica are being developed in our laboratories to produce materials with high conductivity and mechanical stability [54,55,60,63]. The mechanical stability stems from a three-dimensional network of interacting fumed silica aggregates. A unique feature of our CPEs is that the surface chemistry of the fumed silica particles can be tailored to produce desirable mechanical properties without affecting the electrochemical properties. We have investigated composite electrolytes that contain fumed silica with octyl and methacrylate groups on the surface. Composites that contain these dual-functionalized fumed silica can be subsequently reacted to form a chemically crosslinked CPE

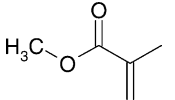
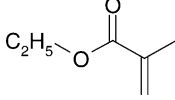
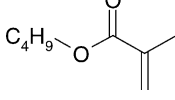
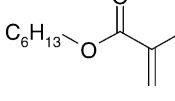
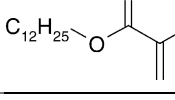
rather than a physically crosslinked CPE [64]. Crosslinked CPEs require the use of additional monomers to form sufficient links between particles to give mechanically robust networks. Ideally, added monomer “coats” the surface of the silica network and provides permanent mechanical stability with minimal penalty in conductivity. Using commercially available crosslinkable fumed silica (Degussa R711) + PEGdm (250) + lithium bis(trifluoromethanesulfonyl)imide (LiTFSI, Li:O = 1:20) + 20 wt.% butyl methacrylate (BMA) monomer, we prepared thermally crosslinked composites with a room-temperature ionic conductivity approaching  $10^{-3} \text{ S cm}^{-1}$  and an elastic modulus [56] ( $G'$ ) approximately  $10^5 \text{ Pa}$ . We have recently built on this preliminary study to examine the effects of fumed silica surface group, fumed silica weight percent, salt concentration, and solvent molecular weight on electrochemical and rheological properties [65]. These composite electrolytes of crosslinked fumed silica exhibit significantly higher elastic modulus and yield stress with minimal penalty in conductivity and ion transport compared to the CPEs with hydrophobic fumed silica. However, these crosslinked systems behaved poorly in lithium–lithium cycling experiments due to the possible presence of unreacted monomer and/or poor interfacial contact.

In this study, we focus on understanding how changes in the monomer bulk properties affect the rheological and electrochemical properties of CPEs using methacrylate monomers of various length and concentration. Results from ionic transport, dynamic rheology, open-circuit interfacial stability, and lithium/lithium cell-cycling are discussed in terms of a mechanistic crosslinking model. In addition, these results are correlated with the bulk properties of the material components to further evaluate the performance of the composites, especially the interfacial stability with lithium.

## 2. Experimental

Chemicals and preparation used in this study consist of five components: crosslinkable-based fumed silica (Degussa R711), lithium salt (lithium bis(trifluoromethanesulfonyl)imide [ $\text{LiN}(\text{CF}_3\text{SO}_2)_2$ ] (LiTFSI, Li imide, 3M)), poly(ethylene glycol)dimethyl ether (PEGdm,  $M_n = 250$ , Aldrich), methacrylate monomer, and initiator [55,66]. LiTFSI is dried at  $110^\circ\text{C}$  under vacuum ( $\sim 1 \text{ kPa}$ ) for 24 h before use. Fumed silicas are dried at  $90^\circ\text{C}$  under vacuum ( $\sim 1 \text{ kPa}$ ) for 1 week to achieve a water content of 150–200 ppm before transferred to a glove box. PEGdm (250), used for interfacial impedance and lithium–lithium cycle studies, is dried over  $4 \text{ \AA}$  molecular sieves for at least 1 week after the inhibitor (butylated hydroxytoluene, BHT) is removed using an inhibitor-removing column (Aldrich). For conductivity and rheology measurements, PEGdm (250) is dried over  $4 \text{ \AA}$  molecular sieves for at least 1 week. Methacrylate monomers with varying length of alkyl chains, methyl (MMA), ethyl (EMA), butyl (BMA), *n*-hexyl (HMA),

Table 1  
Structure and properties of methacrylate monomers used in this study

Monomer	Structure	MW (g mol <sup>-1</sup> )	BP (°C)
Methyl methacrylate (MMA)		100.12	100
Ethyl methacrylate (EMA)		114.14	119
Butyl methacrylate (BMA)		142.20	160
<i>n</i> -Hexyl methacrylate (HMA)		170.24	162
<i>n</i> -Dodecyl methacrylate (DMA)		254.42	192

and *n*-dodecyl (DMA) (Aldrich, Alfa Aesar), are processed through inhibitor-removing columns (Aldrich) to remove monomethyl ether hydroquinone (MEHQ), and then stored over 4 Å molecular sieves in a refrigerator (1 °C). The structure and physical properties of the methacrylate monomers are shown in Table 1. The free-radical initiator, 2,2'-azo-bis-isobutyronitrile (AIBN, Aldrich), is stored in a refrigerator (1 °C) and used as received.

After the appropriate amount of PEGdm electrolyte solution, e.g., LiTFSI in PEGdm (250), is added to the fumed silica, a solution of 1% 2,2'-azo-bis-isobutyronitrile (AIBN) in monomer is added to prepare composites with the desired weight percent of monomer. Samples used in electrochemical measurements are prepared in a glove box and mixed using a high-shear mixer (Tissue Tearor™, Model 398, BioSpec Products Inc.) while samples for rheology are prepared outside the glove box and mixed using a Silverson™ Model SL2 mixer (Silverson Machines). The final CPEs are obtained by curing the samples in a sealed vial inside an oven at 80 °C for 24 h.

### 2.1. Electrochemical characterization

Electrolyte conductivities are measured using a glass conductivity cell that consists of two blocking platinum wire electrodes (0.64 mm diameter, Fisher Scientific) [67]. Conductivity is measured using EG&G Princeton Applied Research PowerSine software to control an EG&G Model 273 potentiostat and an EG&G Model 5210 lock-in amplifier in the frequency range 100–1000 mHz. Cells are calibrated at 25 °C using a standard KCl solution (1409 μS cm<sup>-1</sup> at 25 °C). Conductivity cells are placed in wells in an insulated aluminum block with an internal coolant circuit connected

to a temperature-controlled circulating water bath (Isotope 1016P Fisher Scientific) [54]. The temperature of the water bath is varied from 0 to 100 °C (±1 °C) and the temperature of each sample is measured using a T-type thermocouple placed in a sealed glass compartment fully submerged in the sample. The temperature data acquisition system consists of a National Instruments Fieldpoint Module (FP 1000) connected to two National Instruments eight-channel thermocouple modules (FP-TC-120). The resistivity of the electrolyte is determined by the real-axis intercept on a Nyquist plot. For each sample, multiple cells (typically 3–5) are measured, with the reported value representing the average.

The compatibility between the electrolyte and lithium metal at room temperature is studied by time-dependent impedance spectroscopy using symmetric lithium/CPE/lithium button cells. The crosslinked CPE is prepared by placing the pre-cured composite in a 25.4 mm diameter propylene mesh material (~0.3 mm thick, 50% porosity, McMaster-Carr). The CPE/mesh sample is positioned between two Teflon discs to ensure uniform sample thickness, sealed in a stainless steel vial, and then cured in an oven at 80 °C for 24 h. From this CPE/mesh sample, 12.7 mm diameter discs are punched and used in the fabrication of symmetric lithium/CPE/lithium cells. The design of the button cells is given elsewhere [56]. The cell is stored at open-circuit and room-temperature between and during experiments. The impedance of the cell is measured using EG&G Princeton Applied Research PowerSine software to control an EG&G Model 273 potentiostat and an EG&G Model 5210 lock-in amplifier in the frequency range 100 kHz to 100 mHz. The interfacial resistance between the electrolyte and lithium metal is determined according to the method of Fauteux [1]. For each sample, three cells are prepared and measured. An Arbin battery cycler (Model BT2042) controlled by Arbin ABTS software is employed to carry out constant-current cell cycling using symmetric lithium/CPE/lithium button cells. Current densities of 0.2 mA cm<sup>-2</sup> are applied with a fixed charge density of 1 C cm<sup>-2</sup>, and cell cycling is terminated upon reaching a cell voltage of 500 mV.

### 2.2. Rheological characterization

The dynamic rheology of the crosslinked samples is measured using a TA Instruments AR2000 stress-controlled rheometer. Unless otherwise noted, the temperature of the samples is maintained at 25 °C using a Peltier plate. A 20 mm diameter steel parallel-plate geometry is used on all samples. Sandpaper is adhered to the plate surface to eliminate sample wall-slip, which could result in underestimation of the measured properties of a sample [68]. Samples with a thickness of 800–1500 μm are used. Initially, samples are loaded in a manner to maintain a normal force of less than 5 N on the sample. At the desired thickness, the normal force is allowed to relax below 3 N prior to measurement. For each sample, a dynamic stress sweep is used to determine

the range of stresses within the linear-viscoelastic (LVE) region. A new sample is then loaded and a frequency sweep of  $0.01\text{--}100\text{ rad s}^{-1}$  is performed using a pre-determined LVE stress, followed by a dynamic stress sweep at a constant frequency of  $1\text{ rad s}^{-1}$ . Reported data represent the average of three measurements. Typical experimental variances are less than 20%.

Dynamic rheology measures the elastic ( $G'$ ) and viscous ( $G''$ ) moduli of a sample. The frequency dependence of  $G'$  and  $G''$  is an important indicator of microstructure. The elastic modulus  $G'$  qualitatively provides information about the elastic nature of the material while the viscous modulus  $G''$  qualitatively provides information about the viscous nature of the material. Typically, the frequency dependence of  $G'$  and  $G''$  is measured to understand the extent of structure formation within the sample. For disperse systems with no particle flocculation,  $G''$  is typically greater than  $G'$  over the entire range of frequencies. Moreover, both moduli strongly depend on frequency. For weakly flocculated systems, the presence of particle structures introduces both viscous and elastic effects into the rheological response. Thus, the moduli show a weaker dependence on frequency, and the elastic modulus  $G'$  often exceeds the viscous modulus  $G''$  at high frequencies. If the particles flocculate into a volume-filling network structure, the moduli,  $G'$  and  $G''$  are independent of frequency, and the material is classified as a gel, i.e., shows predominantly elastic properties [69] with  $G' > G''$ .

### 3. Results and discussion

#### 3.1. Effect of monomer weight percent

Crosslinkable fumed silica-based composite polymer electrolytes require the addition of monomer to tether adjacent fumed silica particles together and form a robust solid electrolyte. The addition of monomer to the composite electrolyte can significantly affect the electrochemical and rheological properties. To understand how the amount of monomer influences conductivity, we measured conductivity as a function of monomer weight percent. Fig. 1 shows the conductivity of crosslinked CPEs consisting of 10% R711 in PEGdm (250) + LiTFSI (Li:O = 1:20) with varying amounts of BMA. The conductivity decreases with the amount of BMA present, with 20% BMA resulting in a reduction of a factor of 2 and 40% BMA resulting in a factor of 3 reduction from that in its absence. The addition of BMA does not appear to affect the mechanism of ionic transport since all curves show similar curvature, i.e., the apparent activation energy is unaffected. In general, the mechanism of ionic transport in these crosslinkable-based fumed silica composites indicate that crosslinking reactions occur at a length scale between adjacent silicas thereby unaffected the bulk transport processes of the electrolyte.

The dynamic frequency spectra of crosslinked electrolytes containing 10% R711 in PEGdm (250) + LiTFSI (1:20) with

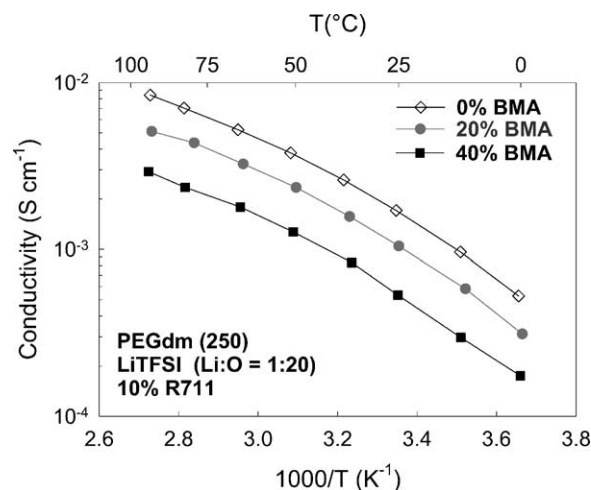


Fig. 1. Effect of monomer weight percent on conductivity of crosslinked CPEs.

BMA monomers at various weight percent (5, 10, 20, and 40 wt.%) are shown in Fig. 2. All samples exhibit higher elastic modulus  $G'$  than viscous modulus  $G''$  (shown only for 5 wt.% BMA for purposes of clarity) at all measured frequencies and exhibit weak frequency dependence, suggesting an elastic network structure [55,56,60,63]. There is a six order of magnitude increase in elastic modulus as the BMA concentration increases from 0 to 5 wt.% BMA. The elastic modulus of crosslinked composites increases with BMA concentration (5–40 wt.%), with a three-fold increase in elastic modulus from 10 to 20 wt.% BMA and no significant change in elastic modulus from 20 to 40 wt.% BMA.

Fig. 3 summarizes the elastic modulus ( $\omega = 1\text{ rad s}^{-1}$ ) and conductivity ( $T = 25\text{ }^\circ\text{C}$ ) of crosslinked composites as a function of BMA weight percent. We find that the crosslinkable-based fumed silica composites possess high conductivity and good mechanical properties. The addition and reaction of 20% BMA increases the elastic moduli over

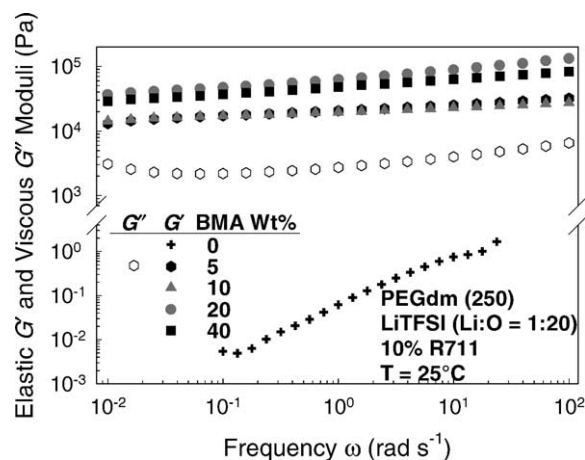


Fig. 2. Effect of monomer weight percent on the elastic and viscous moduli of crosslinked CPEs.

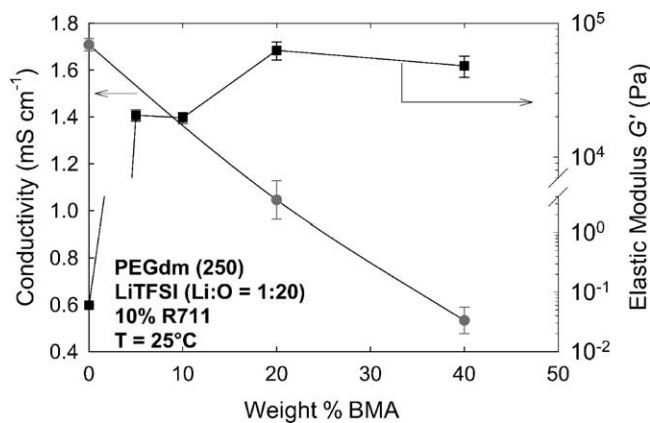


Fig. 3. Conductivity ( $T = 25^\circ\text{C}$ ) and elastic modulus ( $\omega = 1 \text{ rad s}^{-1}$ ) as a function of BMA weight percent after crosslinking.

six orders of magnitude, yet the conductivity decreases only a factor of 2. Such a significant increase in elastic modulus with only a small change in conductivity indicates that the coupling between ionic transport and mechanical strength is weak.

To assess the reactivity of the crosslinked CPEs with lithium metal, cycling of Li/CPE/Li cells is performed. Fig. 4 shows the ohmically corrected average half-cycle voltage versus cycle number for CPEs with various monomer weight percent (0, 5, 10, 20, and 40 wt.% BMA). The results indicate that the amount of BMA in the crosslinked CPEs has a strong influence on cell voltage. The addition of 5, 20, and 40 wt.% BMA and subsequent crosslinking results in higher cell voltage and poorer lithium cycling performance than composites without monomer (no crosslinking). However, the crosslinked CPE containing 10 wt.% BMA exhibits a comparable cell voltage to the sample without monomer. This suggests that crosslinked CPEs can be stable with respect to lithium during charge/discharge cycles.

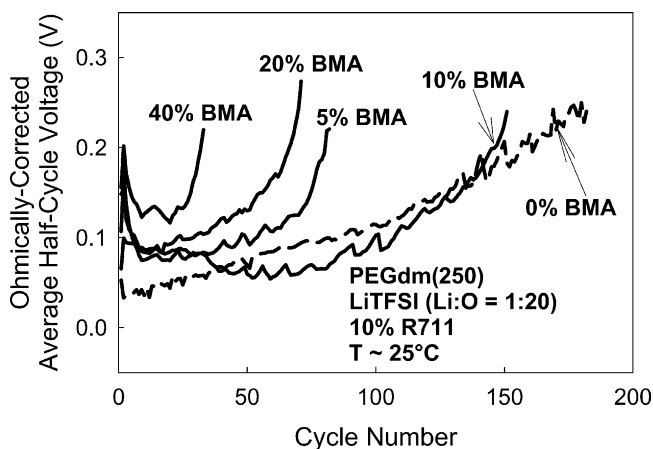


Fig. 4. Cell voltage of Li/CPE/Li cell as a function of cycle number for crosslinked CPEs with four different monomers of varying BMA weight percent.

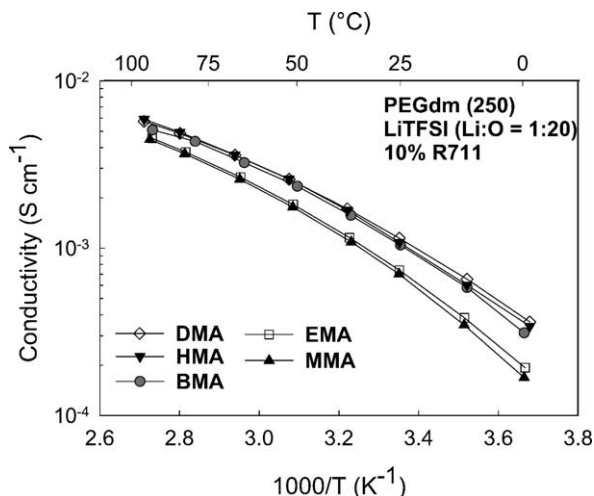


Fig. 5. Conductivity as a function of temperature of CPEs with five different monomers having varying length of alkyl chains.

### 3.2. Effect of monomer alkyl chain length

In addition to varying the amount of monomer, different types of methacrylate monomers are also studied. We chose methacrylate monomers with varying length of alkyl chain lengths to further probe how the chemical nature of the monomer affects the electrochemical and rheological properties. Fig. 5 shows the conductivity of CPEs after crosslinking as a function of temperature for composites with five different monomers (MMA, EMA, BMA, HMA, DMA) at a constant salt concentration (Li:O = 1:20), 20 wt.% monomer, and 10 wt.% R711. The conductivity increases modestly with alkyl chain length, but with a more pronounced change from EMA to BMA. This result is primarily due to the lower solubility of the longer alkyl chains in the PEGdm (250) electrolyte. Longer alkyl monomers are less likely to homopolymerize in the bulk electrolyte phase and are more likely to react at the fumed silica surface to create links between silica particles. Polymerization of the monomer in the electrolyte phase increases the viscosity of the electrolyte thereby impeding ionic transport. The electrolytes containing 20% HMA and 20% DMA have conductivities exceeding  $10^{-3} \text{ S cm}^{-1}$  at room temperature.

The dynamic frequency spectra of crosslinked electrolytes containing 10 wt.% R711 in PEGdm (250) + LiTFSI (1:20) with different monomers at 20 wt.% are shown in Fig. 6. For all samples,  $G'$  exceeds  $G''$ , in addition, both  $G'$  and  $G''$  exhibit only a slight frequency dependence indicating presence of an elastic network. The length of the alkyl segment of the monomer affects the mechanical properties. As the number of alkyl carbons increases, there is an initial increase in elastic modulus that reaches a maximum for samples containing HMA. Further increases in the alkyl chain, e.g., DMA, yield a slightly lower elastic modulus, although the decrease in elastic modulus compared to BMA and HMA may not be significant. This is illustrated more clearly in Fig. 7 which

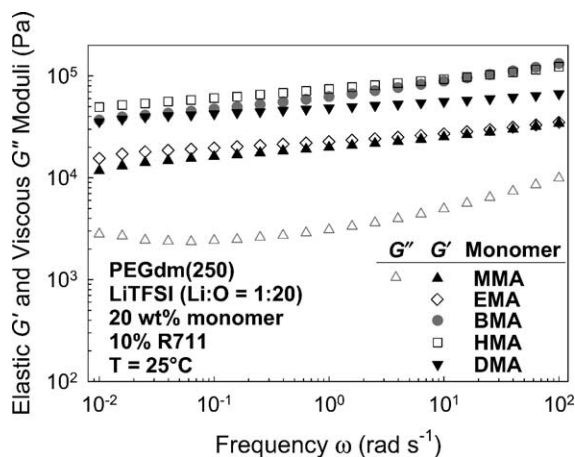


Fig. 6. Effect of varying length of monomer alkyl chain on elastic and viscous moduli.

shows  $G'$  ( $\omega = 1 \text{ rad s}^{-1}$ ) and conductivity ( $T = 25^\circ\text{C}$ ) as a function of alkyl chain length at 20 wt.% monomer. This plot shows that conductivity and elastic modulus exhibit slight increases between MMA and EMA and sharp increases from EMA to BMA followed by moderate changes for HMA and DMA. These crosslinked CPEs are unique in that increasing the alkyl chain length of the monomer enhances both conductivity and elastic modulus. Monomers that tend to polymerize in the interstitial electrolyte phase, such as MMA and EMA, cannot form covalent crosslinks between silica particles. Samples containing such monomers will thus have weaker mechanical properties and lower ionic conductivity than those containing monomers, such as BMA, HMA, and DMA, that do not polymerize in the interstitial electrolyte phase and segregate to the silica surface and react to form covalent crosslinks between silica particles. Using DMA monomer instead of MMA increases the conductivity by 50% and increases the elastic modulus an order of magnitude.

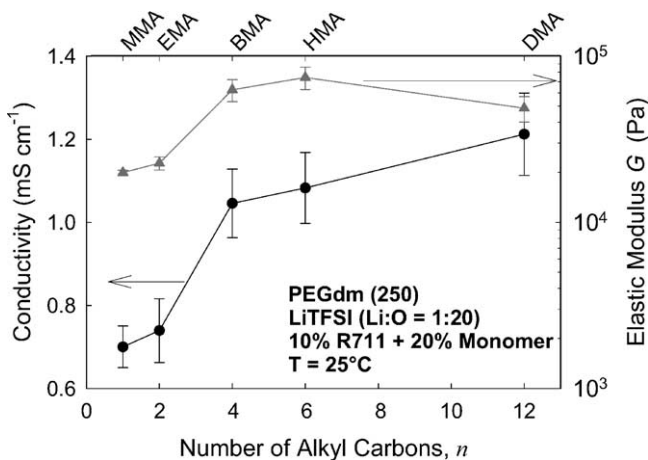


Fig. 7. Conductivity ( $T = 25^\circ\text{C}$ ) and elastic modulus ( $\omega = 1 \text{ rad s}^{-1}$ ) as a function of number of alkyl carbons in the methacrylate monomer.

The addition of fumed silica stabilizes the interface between lithium metal and salt solutions consisting of PEGdm (250) + LiTFSI (Li:O = 1:20) [54,70]. However, crosslinked CPEs are prepared with monomer, initiator, and methacrylate-modified fumed silica that can react with lithium resulting in the formation of a passivating layer on its surface. Open-circuit interfacial impedance measurements are performed to assess the effect of various monomers on the crosslinked CPE interfacial stability with lithium. Fig. 8 shows the open-circuit interfacial impedance of lithium in contact with 10 wt.% R711 in PEGdm (250) + LiTFSI (Li:O = 1:20) (uncrosslinked) with five different monomers at 20 wt.% as a function of time. We find that the interfacial impedance of CPEs without monomer (uncrosslinked) is  $\sim 700 \Omega \text{ cm}^2$  after 60 days. This value is higher than similar CPEs with octyl-modified fumed silica (e.g., Degussa R805) [54]. Although the higher impedance may indicate that the methacrylate surface groups are themselves reactive with lithium metal, the 10 wt.% R711 CPE is liquid-like and stronger gel electrolytes, such as octyl-modified (Degussa R805) fumed silica in PEGdm electrolytes, have lower interfacial impedance than weaker gels [70]. In addition, Fig. 8 shows that the interfacial impedance does not correlate with the length of the alkyl chain in the monomer: EMA, DMA, and MMA exhibit interfacial impedance values significantly higher than the CPE without monomer while BMA and HMA have stable interfacial impedances that are slightly lower than the CPE without monomer. To further assess the reactivity of the crosslinked CPEs with lithium metal, cycling of Li/CPE/Li cells is performed. Fig. 9 shows the ohmically corrected average half-cycle voltage versus cycle number for CPEs with various monomers at 20 wt.% (MMA is not shown since it failed upon the first cycle). The results indicate that the crosslinked CPEs perform poorly than CPEs without monomer at this added level of monomer (compare with 10 wt.% BMA, Fig. 4). In addition, the performance of the crosslinked CPEs is not sensitive to monomer type. EMA composites, which exhibit relatively

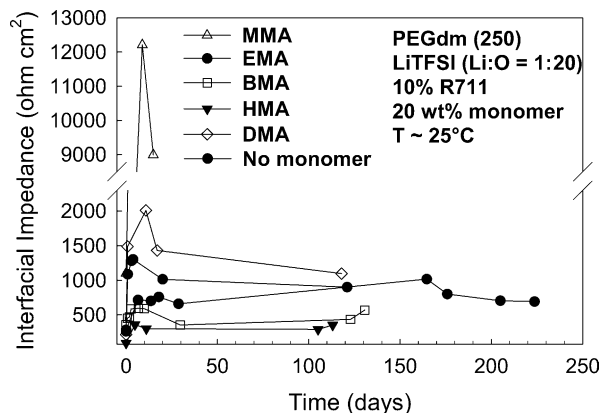


Fig. 8. Open-circuit interfacial impedance as a function of time of crosslinked CPEs with five different monomers of varying alkyl chain length.

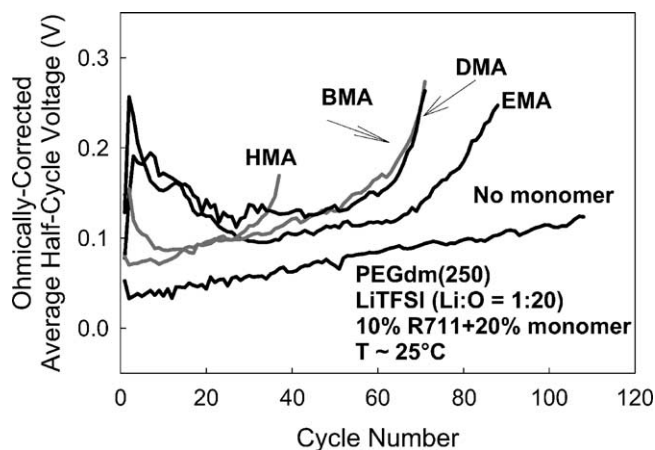


Fig. 9. Cell voltage of Li/CPE/Li cell as a function of cycle number for crosslinked CPEs with four different monomers of varying alkyl chain length.

poor open-circuit interfacial stability, perform the best in cycling studies of Li/CPE/Li cells. Although HMA and BMA have lower interfacial impedance than the CPE without monomer (Fig. 8), both CPEs exhibit higher half-cell voltage and exceed the cut-off voltage much faster than the control. The CPEs without monomer outperforming crosslinked CPEs suggests that impurities, especially unreacted monomer, produce a passivating film on the lithium surface that increases the voltage between the electrodes. Developing protocols to mitigate and/or remove residual monomer are still underway.

#### 4. Summary and conclusions

CPEs containing crosslinkable fumed silica using different methacrylate monomers have been prepared and characterized. The conductivity of the crosslinked CPEs increases as the length of the alkyl chain of the monomer increases with  $\text{DMA} > \text{HMA} > \text{BMA} > \text{EMA} > \text{MMA}$ . The rheological properties of the crosslinked CPEs also depend on the length of the alkyl chain. Longer alkyl chain monomers, such as BMA, HMA, and DMA, have higher elastic moduli than short alkyl chain monomers, such as MMA and EMA. Increases in monomer weight percent result in decreased conductivity, but improved mechanical properties. Crosslinked CPEs containing HMA and BMA exhibit improved interfacial stability relative to CPEs containing no monomer. However, cycling of Li/CPE/Li cells indicate that CPEs containing crosslinked monomer are more reactive with lithium than CPEs without monomer. These results suggest that the location of the reacting monomer is critical. In order to promote high-elastic modulus and high-ionic conductivity, the monomer must react at the fumed silica surface and not in the bulk electrolyte. Furthermore, the crosslinking reaction must consume all the monomer so that residual monomer cannot react with lithium during cycling.

#### Acknowledgements

The authors gratefully acknowledge funding from the Department of Energy, Office of Basic Energy Sciences and Office of FreedomCAR Vehicle Technologies. In addition, we acknowledge the US Department of Education Graduate Assistance in Areas of National Need (GAANN) Fellowship for providing additional funding. We also thank Degussa for providing the fumed silica and 3M for providing the LiTFSI salt.

#### References

- [1] D. Fauteux, A. Massucco, M. McLin, M. Vanburen, J. Shi, *Electrochim. Acta* 40 (1995) 2185.
- [2] W.H. Meyer, *Adv. Mater.* 10 (1998) 439.
- [3] K.L. Heitner, *J. Power Sour.* 89 (2000) 128.
- [4] Z.C. Zhang, S.B. Fang, *Electrochim. Acta* 45 (2000) 2131.
- [5] M. Armand, *Solid State Ionics* 69 (1994) 309.
- [6] R.J. Brodd, W.W. Huang, J.R. Akridge, *Macromol. Symp.* 159 (2000) 229.
- [7] P.G. Bruce, C.A. Vincent, *J. Chem. Soc., Faraday Trans.* 89 (1993) 3187.
- [8] H.J. Gores, J.M.G. Barthel, *Pure Appl. Chem.* 67 (1995) 919.
- [9] F.M. Gray, *Solid Polymer Electrolytes: Fundamentals and Technological Applications*, VCH, Cambridge, UK, 1991.
- [10] F.M. Gray, *Polymer Electrolytes*, Springer Verlag, 1997.
- [11] J.Y. Song, Y.Y. Wang, C.C. Wan, *J. Power Sour.* 77 (1999) 183.
- [12] H.R. Allcock, R. Ravikiran, S.J.M. Oconnor, *Macromolecules* 30 (1997) 3184.
- [13] R. Koksang Olsen II, D. Shackle, *Solid State Ionics* 69 (1994) 320.
- [14] W. Wieczorek, Z. Florjanczyk, J.R. Stevens, *Electrochim. Acta* 40 (1995) 2251.
- [15] O. Buriez, Y.B. Han, J. Hou, J.B. Kerr, J. Qiao, S.E. Sloop, M.M. Tian, S.G. Wang, *J. Power Sour.* 89 (2000) 149.
- [16] C.A. Angell, C. Liu, E. Sanchez, *Nature* 362 (1993) 137.
- [17] Y.T. Kim, E.S. Smotkin, *Solid State Ionics* 149 (2002) 29.
- [18] R. Huq, R. Koksang, P.E. Tonder, G.C. Farrington, *Electrochim. Acta* 37 (1992) 1681.
- [19] S. Izuchi, S. Ochiai, K. Takeuchi, *J. Power Sour.* 68 (1997) 37.
- [20] M.C. Borghini, M. Mastragostino, A. Zanelli, *Electrochim. Acta* 41 (1996) 2369.
- [21] Y.K. Kang, H.J. Kim, E. Kim, B. Oh, J.H. Cho, *J. Power Sour.* 92 (2001) 255.
- [22] S.I. Moon, C.R. Lee, B.S. Jin, K.E. Min, W.S. Kim, *J. Power Sour.* 87 (2000) 223.
- [23] A. Noda, M. Watanabe, *Electrochim. Acta* 45 (2000) 1265.
- [24] C. A. Angell, V. Liu, E. Sanchez, A new type of cation-conducting rubbery solid electrolyte: the ionic rubber, in: *Proceedings of the Symposium of the Materials Research Society*, vol. 293, San Francisco, CA, 12–16 April 1993, p. 75.
- [25] A. Zalewska, I. Pruszczyk, E. Sulek, W. Wieczorek, *Solid State Ionics* 157 (2003) 233.
- [26] C.S. Kim, S.M. Oh, *Electrochim. Acta* 45 (2000) 2101.
- [27] H.S. Choe, B.G. Carroll, D.M. Pasquariello, K.M. Abraham, *Chem. Mater.* 9 (1997) 369.
- [28] K.M. Abraham, Z. Jiang, B. Carroll, *Chem. Mater.* 9 (1997) 1978.
- [29] F. Croce, F. Gerace, G. Dautzemberg, S. Passerini, G.B. Appetecchi, B. Scrosati, *Electrochim. Acta* 39 (1994) 2187.
- [30] K.M. Abraham, M. Alamgir, *J. Power Sour.* 43 (1993) 195.
- [31] S.R. Starkey, R. Frech, *Electrochim. Acta* 42 (1997) 471.
- [32] F. Croce, S.D. Brown, S.G. Greenbaum, S.M. Slane, M. Salomon, *Chem. Mater.* 5 (1993) 1268.

- [33] B.Y. Huang, Z.X. Wang, L.Q. Chen, R.J. Xue, F.S. Wang, *Solid State Ionics* 91 (1996) 279.
- [34] G.B. Appetecchi, F. Croce, B. Scrosati, *Electrochim. Acta* 40 (1995) 991.
- [35] F. Croce, G.B. Appetecchi, L. Persi, B. Scrosati, *Nature* 394 (1998) 456.
- [36] F. Capuano, F. Croce, B. Scrosati, *J. Electrochem. Soc.* 138 (1991) 1918.
- [37] J.E. Weston, B.C.H. Steele, *Solid State Ionics* 7 (1982) 75.
- [38] B. Scrosati, *J. Electrochem. Soc.* 136 (1989) 2774.
- [39] J. Plochanski, W. Wiczorek, *Solid State Ionics* 28 (1988) 979.
- [40] F. Croce, B. Scrosati, G. Mariotto, *Chem. Mater.* 4 (1992) 1134.
- [41] W. Gang, J. Roos, D. Brinkmann, F. Capuano, F. Croce, B. Scrosati, *Solid State Ionics* 53–56 (1992) 1102.
- [42] W. Wiczorek, *Mater. Sci. Eng. B* 15 (1992) 108.
- [43] F. Croce, S. Passerini, A. Selvaggi, B. Scrosati, *Solid State Ionics* 40–41 (1990) 375.
- [44] M.C. Borghini, M. Mastragostino, S. Passerini, B. Scrosati, *J. Electrochem. Soc.* 142 (1995) 2118.
- [45] W. Wiczorek, K. Such, Z. Florjanczyk, J.R. Stevens, *J. Phys. Chem.* 98 (1994) 6840.
- [46] W. Wiczorek, K. Such, H. Wycislik, J. Plochanski, *Solid State Ionics* 36 (1989) 255.
- [47] B. Kumar, L.G. Scanlon, *Solid State Ionics* 124 (1999) 239.
- [48] F. Croce, R. Curini, A. Martinelli, L. Persi, F. Ronci, B. Scrosati, R. Caminiti, *J. Phys. Chem. B* 103 (1999) 10632.
- [49] Y.P. Ma, M. Doyle, T.F. Fuller, M.M. Doeff, L.C. Dejonghe, J. Newman, *J. Electrochem. Soc.* 142 (1995) 1859.
- [50] G.B. Appetecchi, F. Croce, P. Romagnoli, B. Scrosati, U. Heider, R. Oesten, *Electrochem. Commun.* 1 (1999) 83.
- [51] M. Kono, M. Nishiura, E. Ishiko, T. Sada, *Electrochim. Acta* 45 (2000) 1307.
- [52] M. Kono, E. Hayashi, M. Nishiura, M. Watanabe, *J. Electrochem. Soc.* 147 (2000) 2517.
- [53] Y. Saito, C. Capiglia, H. Yamamoto, P. Mustarelli, *J. Electrochem. Soc.* 147 (2000) 1645.
- [54] J. Fan, P.S. Fedkiw, *J. Electrochem. Soc.* 144 (1997) 399.
- [55] J. Fan, S.R. Raghavan, X.Y. Yu, S.A. Khan, P.S. Fedkiw, J. Hou, G.L. Baker, *Solid State Ionics* 111 (1998) 117.
- [56] H.J. Walls, J. Zhou, J.A. Yerian, P.S. Fedkiw, S.A. Khan, M.K. Stowe, G.L. Baker, *J. Power Sour.* 89 (2000) 156.
- [57] S.R. Raghavan, S.A. Khan, *J. Rheol.* 39 (1995) 1311.
- [58] S.R. Raghavan, G.W. Fussell, S.A. Khan, *Abstr. Pap. Am. Chem. Soc.* 214 (1997) 332.
- [59] S.R. Raghavan, S.A. Khan, *J. Colloid Interface Sci.* 185 (1997) 57.
- [60] S.R. Raghavan, M.W. Riley, P.S. Fedkiw, S.A. Khan, *Chem. Mater.* 10 (1998) 244.
- [61] S.R. Raghavan, J. Hou, G.L. Baker, S.A. Khan, *Langmuir* 16 (2000) 1066.
- [62] S.R. Raghavan, H.J. Walls, S.A. Khan, *Langmuir* 16 (2000) 7920.
- [63] S.A. Khan, G.L. Baker, S. Colson, *Chem. Mater.* 6 (1994) 2359.
- [64] J. Hou, G.L. Baker, *Chem. Mater.* 10 (1998) 3311.
- [65] J. Yerian, Ph.D. Dissertation, NC State University, 2003.
- [66] J. Hou, *Composite Polymer Electrolytes Using Functionalized Fumed Silica and Low Molecular Weight PEO: Synthesis and Characterization*, Michigan State University, Lansing, MI, 1997.
- [67] M. Riley, P.S. Fedkiw, S.A. Khan, *J. Electrochem. Soc.* 149 (2002) A667.
- [68] R. Buscall, J.I. McGowan, A.J. Mortonjones, *J. Rheol.* 37 (1993) 621.
- [69] C.W. Macosko, *Rheology: Principles, Measurements and Applications*, VCH, New York, NY, 1994.
- [70] J. Zhou, P.S. Fedkiw, S.A. Khan, *J. Electrochem. Soc.* 149 (2002) A1121.